DFT Study of Zeolite LTA Structural Fragments: Double Four-Member Rings of Oxygen-Bridged Silicon and Aluminum Atoms

Ellie L. Uzunova and Georgi St. Nikolov*

Institute of General and Inorganic Chemistry, Bulgarian Academy of Sciences, Sofia 1113, Bulgaria

Received: October 28, 1999; In Final Form: March 20, 2000

The electronic structure and relative stability of $[H_8Si_{8-x}Al_xO_{12}]^{x-}$ structural fragments with Si and Al atoms located at tetrahedral sites and connected by bridging oxygen atoms so as to form a tetragonal prism, together with oxygen-coordinated charge-compensating cations, are studied by the B3LYP/6-31G(d) method. Clusters with Al/Si ratios in the 0−1 range and different orderings of the extraframework cations and Si and Al at tetrahedral sites are proper models for the double four-member rings, which are secondary building units of the LTA structure. The stability of the structure fragments is higher when the framework's negative charges are at maximum distance, in agreement with Dempsey's rule. The HOMO orbitals of $H_8Si_8O_{12}$, the anionic clusters $[H_8Si_{8-x}Al_xO_{12}]^{x-}$, and the proton-balanced ones are mainly O 2p nonbonding AO. In fragments with Al/Si > 0 and Na^+ at extraframework cation positions, the oxygen nonbonding nature of the HOMO orbital decreases and certain electron density is shifted to the Al centers. The LUMO orbitals of $Na_xH_8Si_{8-x}Al_xO_{12}$ clusters consist of the charge-balancing cations' AO.

Introduction

Cyclic polysiloxanes, $H_{2n}T_nO_n$, built from oxygen-bridged tetrahedral Si atoms readily polymerize further to either 2D sheet silicates or to 3D fragments (double rings and cages) that are the secondary building units of zeolite structures.[1] The lower members of the $H_{2n}T_nO_n$ family ($n < 4$) are expected to experience considerable strain; nevertheless, the $H_4Si_2O_2$ unit has been isolated and studied both theoretically and experimentally.[2,3] Rings with more than four tetrahedral atoms are very flexible and they exist in many conformations with rather close energies. In aluminosilicates, Al substitutes Si atoms at tetrahedral sites and the negative charge is compensated either by a proton or by an extraframework cation. Cage-shaped hydrosilasesquioxanes are more stable than the ring fragments and they exist in much more rigid architectures.[4,5] They are of the general formula $(HSiO_{3/2})_{2n}$, where $n = 2$, 3, etc., and those with $n =$ 4, 6, and 8 correspond to zeolite secondary building units: double four-member rings (D_4R) with eight tetrahedral atoms are secondary building units in LTA zeolites and the mineral gismondine.[6,7] An alumosilasesquioxane D_4R with Si/Al = 1 and $4Na^+$ at positions nearly centered opposite to a four-member ring window has been synthesized.[8] The cage-shaped structures have been subjected to many theoretical and experimental studies.[4−13] The reactivity of substituted double four-member rings ($X_8Si_8O_{12}$; X = H, Cl, CH_3) has been modeled by the Extended Huckel method, [9] and the stability of anionic species with different levels of Si/Al substitution has been studied by the semiempirical AM1 method.[10] Modeling of the cage-shaped polysiloxanes at the Hartree−Fock level revealed the high stability of cages containing rings with 4, 5, and 6 tetrahedral atoms.[11,12] DFT studies of H-silsesquioxane cages pointed that nonlocal density approximation is required for reliable comparison of isomers.[14]

The aim of the present study is to examine the Si,Al ordering in double four-member rings $H_8T_8O_{12}$ (T = Si, Al) with different Al/Si ratios in the presence of charge-compensating cations, Na^+ or H^+. The stabilization of negatively charged frameworks that result from a particular coordination of the countercations is discussed. The electronic structures of clusters with different charge distributions are analyzed.

Methods

Calculations were performed with the B3LYP exchange−correlation functional, which includes local and nonlocal terms, as implemented in the *Gaussian 98* package.[15−18] The 6-31G(d) basis set was employed; for the fragments containing hydroxyl groups, polarization functions at the hydrogen atoms were included via the 6-31G(d,p) basis. Cartesian coordinates were used in all optimizations with no initial geometry restrictions. Frequency calculations were performed for all of the electroneutral species at their optimized geometry. The absence of negative frequencies was taken as proof that the point reached represents a minimum on the potential energy surface.[19]

Stability of Double Four-Member Rings (D_4R) with Si, Al Substitution. The D_4R models with distinct Si and Al locations at tetrahedral sites are presented in Figure 1 with the symmetry groups resulting from geometry optimizations. Anionic fragments were built by substituting Si for Al in the $H_8Si_8O_{12}$ molecule according to Löwenstein's rule for avoidance of Al−O−Al linkages.[20] The electroneutral species $Na_xH_8Si_{8-x}Al_xO_{12}$ were derived from the anionic fragments by placing the extraframework Na^+ cations at positions with maximum oxygen coordination and centered against T_4O_4 ring faces. These sites correspond to Na(3) in zeolite NaA.[7] The structural parameters of these models are summarized in Table 1. The $H_8Si_8O_{12}$ model geometry corresponds to that of the synthetic molecule.[4] The anionic fragments and the electroneutral species, obtained by adding extraframework charges, have longer Si−O and Al−O bonds and shorter Na−O bonds, compared to the values that are determined experimentally for zeolite A, see Table 1. In all fragments, the O−T−O angles are distorted tetrahedral angles and they vary in a 103−116°

10.1021/jp993827s CCC: $19.00
Published on Web 05/12/2000

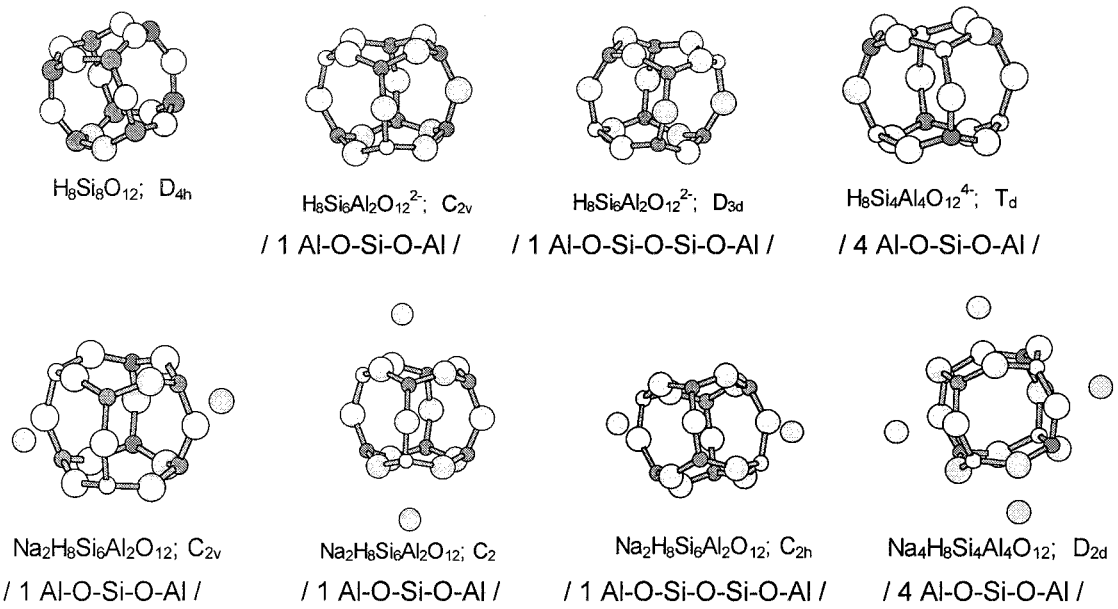

Figure 1. D_4R equilibrium geometry, calculated by the DFT/B3LYP method. Atoms in decreasing size are O, Na^+, tetrahedral Si and Al. Oxygen atoms are light gray circles, Na^+ are gray circles, Si are dark gray small circles, Al are white small circles. The sequence of T-atoms linking is denoted below each model.

TABLE 1: Geometry Parameters of D_4R Fragments, Pictured in Figure 1 and Calculated by B3LYP

prism model	R_{Si-O} (Å)	R_{Al-O} (Å)	∠Al−O−Si (deg)	∠O−Al−O (deg)	∠Si−O−Si (deg)	∠O−Si−O (deg)	R_{Si-H} (Å)	R_{Al-H} (Å)	R_{Na-O} (Å)
D_{4h}; $H_8Si_8O_{12}$	1.64				148	110	1.46		
T_d; $[H_8Si_4Al_4O_{12}]^{4-}$	1.64	1.77	142	112		114	1.53	1.67	
D_{2d}; $Na_4H_8Si_4Al_4O_{12}$	1.65	1.79	137; 152	103; 115		107; 116	1.48	1.59	2.3; 2.55
D_{3d}; $[H_8Si_6Al_2O_{12}]^{2-}$	1.64	1.78	144	108	146	109; 113	1.49	1.60	
C_{2h}; $Na_2H_8Si_6Al_2O_{12}$	1.65	1.78	144	109	136	109	1.47	1.58	2.3; 2.5
C_{2v}; $[H_8Si_6Al_2O_{12}]^{2-}$	1.64	1.78	145	109	155	109−116	1.48	1.62	
C_{2v}; $Na_2H_8Si_6Al_2O_{12}$	1.64	1.79	138	108	135	113	1.47	1.58	2.40
C_2; $Na_2H_8Si_6Al_2O_{12}$	1.65	1.79	135	109	137	109−113	1.48	1.58	2.30−2.55
NaA (exp)[7]	1.59−1.60	1.72−1.74	142−145	106−112		107−111			2.59; 2.61
$Na_4R_8Si_4Al_4O_{12}$(exp)[8]	1.61	1.75		104−116		106−113			2.41; 2.62

range, which is also valid for the experimentally determined angles. In the $Na_4H_8Si_4Al_4O_{12}$ cluster model, the extraframework cation Na^+ forms two shorter and two longer Na−O bonds, similarly to the $Na_4R_8Si_4Al_4O_{12}$ molecule (R-organosilicon substituent),[8] while in zeolite NaA, the Na(3) cations are in almost equivalent oxygen coordination, see Table 1. In the NaA zeolite, the Na(3) site has contacts with two O(1) and two O(3) atoms from the D_4R and it is positioned in the large cage. The interactions with other atoms from the framework and other cation sites are thus limited. Due to the low fractional occupancy of the Na(3) sites, however, the error in the experimentally determined Na−O distances is significant.[7]

The D_4R units within $[H_8Si_6Al_2O_{12}]^{2-}$ (Si/Al = 3), with two Si atoms substituted by two Al atoms, exist in two configurations; they refer to the anionic species with symmetry point group D_{3d} and C_{2v}, respectively. The first one is in agreement with both Löwenstein's[20] and Dempsey's[21] rules, and the second one ignores Dempsey's rule.[21] The structure with maximum separation between the negative charges (D_{3d}; $[H_8Si_6Al_2O_{12}]^{2-}$) is more stable than the other one with simply alternating Si and Al atoms in one T_4O_4 ring (C_{2v}; $[H_8Si_6Al_2O_{12}]^{2-}$), see Table 2.

In the optimization procedure, the charge-compensating extraframework cations, Na^+, take positions so as to confront two opposite Si_3AlO_4 faces in a structure with maximum negative charge separation. The resulting configuration is with

TABLE 2: Relative Energies of D_4R Isomers with Si/Al = 3

prism model[a]	relative energy [b](kJ mol^{-1}) zero-point correction: not included	relative energy [b](kJ mol^{-1}) zero-point correction: included	HOMO−LUMO energy gap (eV)
D_{3d}; $H_8Si_6Al_2O_{12}$ $^{2-}$	0.0		8.2
C_{2v}; $H_8Si_6Al_2O_{12}$ $^{2-}$	21.5		7.9
C_{2h}; $Na_2H_8Si_6Al_2O_{12}$	0.0	0.0	6.4
C_{2v}; $Na_2H_8Si_6Al_2O_{12}$	28.6	28.3	5.5
C_2; $Na_2H_8Si_6Al_2O_{12}$	15.9	15.8	6.2
C_i; $H_8Si_6Al_2O_{10}(OH)_2$	0.0	0.0	8.1
C_{2v}; $H_8Si_6Al_2O_{10}(OH)_2$	29.3	29.6	7.7

[a] The groupings are of compounds with identical composition and different symmetry. [b] The lowest energy within the group is taken as reference zero. The absolute energies of the compounds from the different groups are not comparable because of the different compositions.

lower symmetry, $D_{3d} \Rightarrow C_{2h}$. In the $[H_8Si_6Al_2O_{12}]^{2-}$ anion with C_{2v} symmetry, the negative charges are located within a $Si_2Al_2O_4$ ring. Thus, two distinct configurations emerge with respect to the positions of the two extraframework cations at maximum separation between them: (a) a configuration in which one Na^+ is located so as to confront the $Si_2Al_2O_4$ face and the other Na^+ confronts the opposite Si_4O_4 face, symmetry point group remaining C_{2v}; (b) another configuration with lower symmetry (C_2) is obtained when the two positive charges are positioned against the other two opposite Si_3AlO_4 faces, see

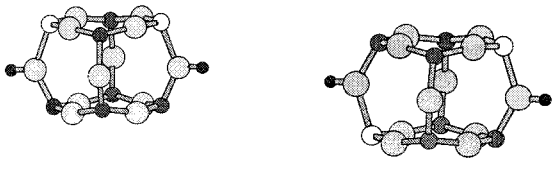

Figure 2. Equilibrium geometry of D_4R with bridging hydroxyl groups $H_8Si_6Al_2O_{10}(OH)_2$, calculated by the B3LYP method. Bridging hydroxyl groups are in the plane of O(1) atoms, referring to the notation of LTA zeolites.[7] Atoms with decreasing size are: O, tetrahedral Si and Al, H. Oxygen atoms are light gray circles, Si are black circles, Al are white circles, H are black small circles.

TABLE 3: Harmonic Stretching Vibrations and Selected Internuclear Distances of Bridging Hydroxyl Groups in Al−(OH)−Si

model	$R_{O(1)-H}$ (Å)	distance Al−HO(1) (Å)	O(1)−H freq cm^{-1}
C_i; $H_8Si_6Al_2O_{10}(OH)_2$	0.97	2.48	3829
C_{2v}; $H_8Si_6Al_2O_{10}(OH)_2$	0.97	2.50	3830
DFT/SMP[a](FAU[c])[22]	0.97	2.46	3723
DFT/LDA [b](FAU)[23]	0.98	2.49	3731
expt[d](FAU)[24]			3787

[a] Shell model potential. [b] Local density approximation. [c] FAU − faujasite. [d] Harmonic frequency, calculated from the experimentally observed anharmonic vibration.

Figure 1. The loss of a vertical symmetry plane σ_v in the $C_{2v} \rightleftharpoons C_2$ transformation results from the peculiar positions of the Na^+ ions. Comparison of the relative energies for the three configurations of general composition $Na_2H_8Si_6Al_2O_{12}$ and different symmetry (C_{2v}, C_2, C_{2h}) reveals that the C_{2h} unit with maximum negative charge separation is the most stable one, the C_2 unit coming next, see Table 2.

Two different electroneutral isomeric fragments with C_{2v} and C_i symmetry, containing isolated bridging hydroxyl groups, Al−OH−Si, were derived from the anions $[H_8Si_6Al_2O_{12}]^{2-}$ with C_{2v} and D_{3d} symmetry by placing H^+ at two opposite Al−O−Si edges, see Figure 2. They were selected among the twelve possible isomers of $H_8Si_6Al_2O_{10}(OH)_2$ as the two forms with noninteracting hydroxyl groups so as to distinguish the role of the cation in stabilizing the two types of Si, Al ordering. The C_{2v} model, $H_8Si_6Al_2O_{10}(OH)_2$, retains the symmetry of the parent anion, while the fragment, resulting from the D_{3d} anion upon hydroxyl group formation, retains only the center of symmetry, $D_{3d} \Rightarrow C_i$. The O(1)−H bond lengths are the same for the C_{2v} and C_i models (0.97 Å); the distance between Al and the H from the bridging OH is slightly longer by 0.02 Å in the model with closely positioned Al centers. The stretching vibrations of the bridging OH are independent of the Si, Al ordering, see Table 3. Protonic forms of the LTA zeolites are unstable, and for that reason the models are hypothetical; the calculated frequencies are compared with data on the bridging O(1)−H group from the hexagonal prism of FAU zeolites. Periodic DFT calculations using a shell model potential [22] and the local density approximation [23] tend to underestimate the stretching OH harmonic frequency, see Table 3;[24] our cluster model B3LYP calculations predict a higher value for the bridging (OH) frequency in a tetragonal prism. The internuclear distances within Al−(OH)−Si, obtained by different methods, vary insignificantly, Table 3.

In all configurations, maximum separation of the negative charges is energetically favored. The energy difference between the isomeric structures with isolated negative charges and the structures with negative charges concentrated in one T_4O_4 ring

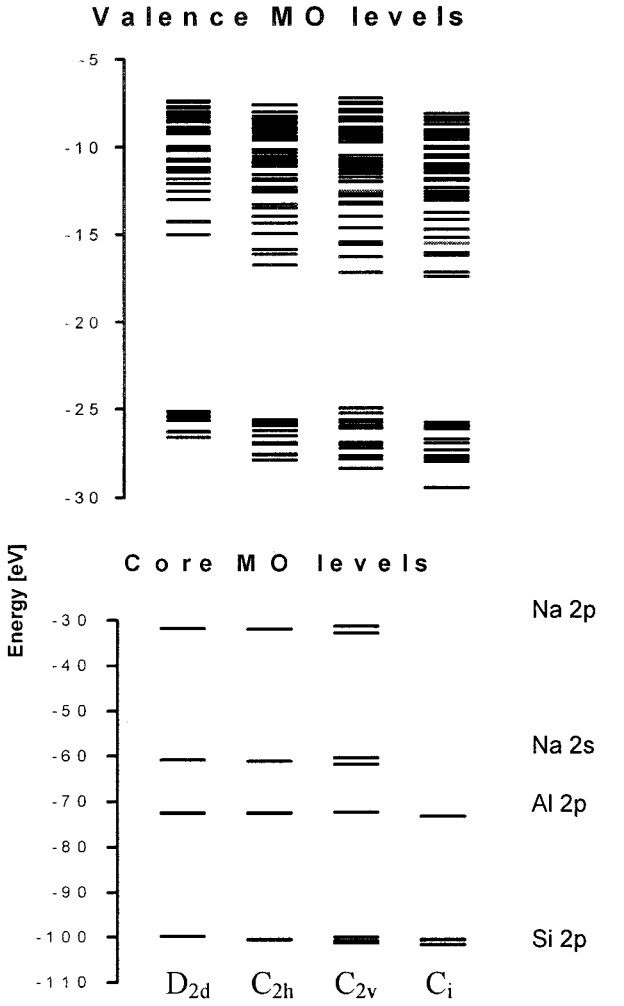

Figure 3. Valence and core MO energies of model fragments: D_{2d}−$Na_4H_8Si_4Al_4O_{12}$; C_{2h}−$Na_2H_8Si_6Al_2O_{12}$; C_{2v}−$Na_2H_8Si_6Al_2O_{12}$; C_i−$H_8Si_6Al_2O_{10}(OH)_2$.

increases in the order: extraframework Na^+ < anion < H^+. The HOMO−LUMO energy gaps follow a similar trend and are lower for structures containing extraframework charges. The zero-point corrections do not change significantly the relative energies of the isomers, since ground states of similar constitutions are compared, see Table 2.

Molecular Orbitals. The D_4R valence MOs form two areas of closely spaced energy levels, see Figure 3. The inner-valence region consists predominantly of MOs from s-AOs. The outer-valence region corresponds to MOs extended over the Si−O, Al−O, and Na−O bonds, with participation of the O 2p, Si 3s, Si 3p, Al 3s, Al 3p, and Na 3s AOs. Broadening of the valence band is observed for the clusters with lower symmetry. The UPS spectral envelope of LTA zeolites and the protonic forms[25−27] are reproduced by the calculations. The calculated core orbital energy levels are in general agreement with data from XPS of zeolites, see Figure 3 and refs 27 and 28. Orbital energy decreases with increasing the Si/Al ratio, mostly for Si and less for Al core levels, in agreement with experiment.[27] The splitting of the Si 2p energy level for D_4R with Si/Al > 1, due to the presence of unequivalent Si atoms, is less than 1 eV.

The HOMO in a Si-only D_4R is of pronounced nonbonding O 2p nature, in agreement with previous assignments.[9,11,14] This feature is retained in all of the anionic Al-containing D_4R and in the clusters with bridging hydroxyl groups, see Figure 4. In D_4R with Na^+ charge-compensating extraframework cations, a

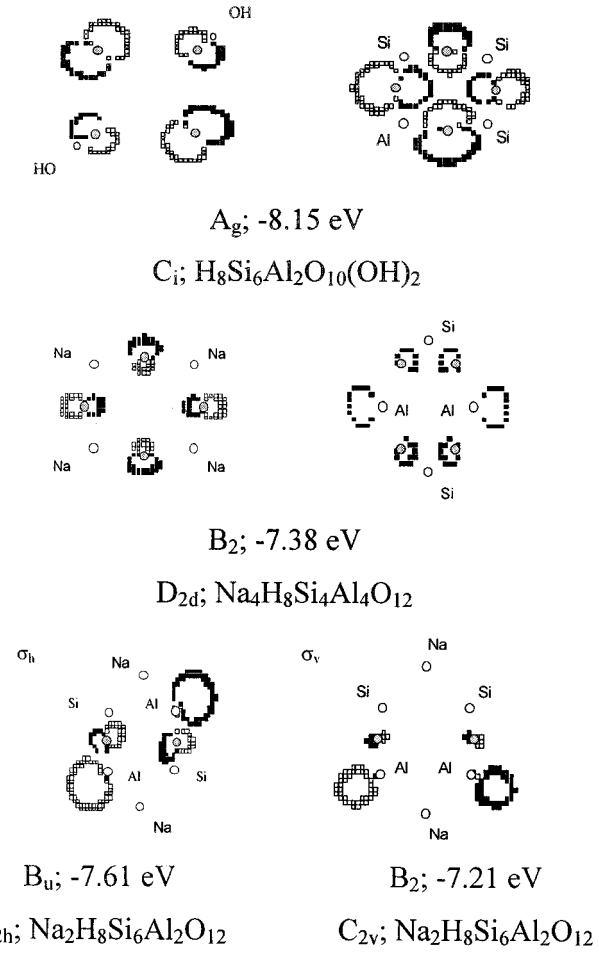

Figure 4. HOMO contour plots. For D_{2d} and C_i fragments, one T_4O_4 face is shown and also the plane defined by four bridging oxygen atoms; for C_{2h} and C_{2v} fragments, the contours are in the denoted symmetry planes. Atom nuclei are represented by opened circles, the oxygen atoms being light gray; the positive parts of the orbitals are depicted by filled squares and the negative part by opened squares. Orbital contours correspond to 90% electron density.

certain part of the electron density is spread over the Al atoms of the framework. These Al atoms are at distances 3.6−3.9 Å from the cations that are longer than those of the oxygen atoms, see Table 1. Comparison of the MO coefficients reveals that the HOMO electron density decreases for oxygen atoms bonded to Al-atoms in a configuration with local concentration of the negative framework charges. This is illustrated in Figure 4: electron density at oxygen atoms decreases in the order C_i > $D_{2d} \geq C_{2h} > C_{2v}$. The cation sites, located at Al-rich T_4O_4 faces are as a result energetically less favorable. The C_{2v} fragment, $Na_2H_8Si_6Al_2O_{12}$, with a $Si_2Al_2O_4$ ring has a broader valence band region and a higher HOMO energy than either the more stable isomer with C_{2h} symmetry or the D_{2d} fragment with higher Al content. The energy difference between the outer- and inner-valence bands is reduced to 7.7 eV, and the HOMO−LUMO energy gap is the lowest for the C_{2v} fragment, see Table 2. The Na 2s and Na 2p energy levels in this particular model are split by 1.5 eV, see Figure 3. The Na 2s and Na 2p orbitals of the cation, positioned against a Si_4O_4 ring are of lower energy than for the opposite cation at the $Si_2Al_2O_4$ ring. The results are consistent with the low fractional occupancy of the Na(3) sites in NaA (ca. 7%). The most populated Na(1) cation sites are located at a six-member ring, coordinated by three oxygen atoms at 2.34 Å with three Al neighbors, placed at less than 3.3 Å from the cation center.

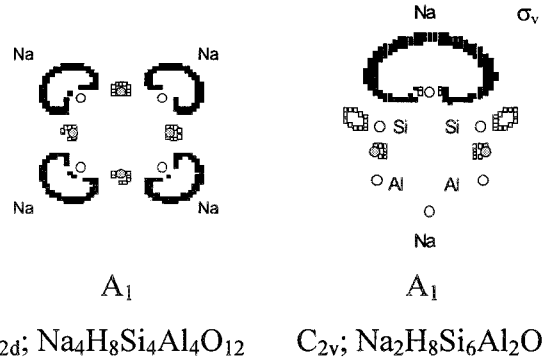

Figure 5. LUMO contour plots (see the legend to Figure 4).

In configurations with Na^+ as extraframework cation, the LUMOs are concentrated mainly at the center of positive charge, as illustrated with the D_{2d} model in Figure 5. In the particular arrangement with C_{2v} symmetry and two unequivalent cations (one near the Al-rich $Si_2Al_2O_4$ face and the other near the Si_4O_4 face), the LUMO is formed from AOs of Na^+ positioned far from the negative charges, see Figure 5, while the next virtual orbital belongs to the less stable cation, located opposite the $Si_2Al_2O_4$ face.

Conclusions

Geometry optimizations by the DFT/B3LYP method of D_4R fragments, $[M^+]_x[H_8Si_{8-x}Al_xO_{12}]^{x-}$ with $x = 0-4$; $M^+ = H^+$, Na^+, reveal that Si,Al orderings with maximum separation of the framework charges are the lowest energy orderings. The composition of the HOMOs and LUMOs is mainly affected by the type of extraframework cations (Na^+ or H^+) and by their locations with respect to the framework structure. Electron density is shifted from the oxygen lone-pair to the Al centers in the $Na_xH_8Si_{8-x}Al_xO_{12}$ fragments. The core orbitals of cations with different number of Al-neighbors are found to be split. Cation sites, located at Al-rich T_4O_4 rings, are coordinatively unsaturated.

Acknowledgment. The authors gratefully acknowledge CPU time from the Computer Center, Technical University, Vienna, where most of the *Gaussian 98* calculations were performed, as well as the assistance with the calculations, kindly provided by Dr. Hans Mikosch from the same university.

References and Notes

(1) Newsam, J. M. In *Solid State Chemistry*: *Compounds*; Cheetham, A. K., Day, P. Eds.; Oxford University Press: **1992**; vol .2, p 234.
(2) Kudo, T.; Nagase, S. *J. Am. Chem. Soc.* **1985**, *107*, 2589.
(3) Fink, M.; Haller, K.; West, R.; Michl, J. *J. Am. Chem. Soc.* **1984**, *106*, 822.
(4) Auf der Heyde, T.; Bürgi, H.-B.; Bürgi, H.; Tornroos, K. *Chimia* **1991**, *45*, 38.
(5) Bürgi, H.-B.; Bürgi, H.; Calzaferri, G.; Tornroos, K. *Inorg. Chem.* **1993**, *32*, 4914.
(6) Smith, J. V. *Chem. Rev.* **1988**, *88*, 149.
(7) Pluth, J. J.; Smith, J. V. *J. Am. Chem. Soc.* **1980**, *102*, 4704.
(8) Montero, M.; Voigt, A.; Teichert, M.; Uson, I.; Roesky, H. *Angew. Chem., Int. Ed. Engl.* **1995**, *34*, 2504.
(9) Calzaferri, G.; Hoffmann R. *J. Chem. Soc., Dalton Trans.* **1991**, 917.
(10) Earley, C. *Inorg. Chem.* **1992**, *31*, 1250.
(11) Earley, C. *J. Phys. Chem.* **1994**, *98*, 8693.
(12) Tossell, J. *Inorg. Chem.* **1998**, *37*, 2223.
(13) Tossell, J. *J. Phys. Chem.* **1996**, *100*, 14828.
(14) Xiang, K.-H.; Pandey, R.; Pernisz, U.; Freeman, C. *J. Phys. Chem. B* **1998**, *102*, 8704.

(15) *Gaussian 98*, Revision A.3, Frisch, M. J.; Trucks, G. W.; Schlegel, H. B.; Scuseria, G. E.; Robb, M. A.; Cheeseman, J. R.; Zakrzewski, V. G.; Montgomery, J. A., Jr.; Stratmann, R. E.; Burant, J. C.; Dapprich, S.; Millam, J. M.; Daniels, A. D.; Kudin, K. N.; Strain, M. C.; Farkas, O.; Tomasi, J.; Barone, V.; Cossi, M.; Cammi, R.; Mennucci, B.; Pomelli, C.; Adamo, C.; Clifford, S.; Ochterski, J.; Petersson, G. A.; Ayala, P. Y.; Cui, Q.; Morokuma, K.; Malick, D. K.; Rabuck, A. D.; Raghavachari, K.; Foresman, J. B.; Cioslowski, J.; Ortiz, J. V.; Stefanov, B. B.; Liu, G.; Liashenko, A.; Piskorz, P.; Komaromi, I.; Gomperts, R.; Martin, R. L.; Fox, D. J.; Keith, T.; Al-Laham, M. A.; Peng, C. Y.; Nanayakkara, A.; Gonzalez, C.; Challacombe, M.; Gill, P. M. W.; Johnson, B.; Chen, W.; Wong, M. W.; Andres, J. L.; Head-Gordon, M.; Replogle, E. S.; and Pople, J. A.; Gaussian, Inc.: Pittsburgh, PA, 1998.

(16) Lee, C.; Yang W.; Parr, R. G. *Phys. Rev.* **1988**, *B37*, 785−789.

(17) Miehlich, B.; Savin, A.; Stoll, H. Preuss, H. *Chem. Phys. Lett.* **1989**, *157*, 200.

(18) Becke, A. D. *J. Chem. Phys.* **1993**, *98*, 5648−5652.

(19) Foresman, J.; Frisch, Æ. In *Exploring Chemistry with Electronic Structure Methods*, 2nd ed.; Gaussian Inc.: Pittsburgh, PA, 1996; Chapter 3.

(20) Löwenstein, W. *Am. Mineral.* **1954**, *39*, 92.

(21) Dempsey, E.; Kuhl, G.; Olson, D. *J. Phys. Chem.* **1969**, *73*, 387.

(22) Sierka, M.; Sauer, J. *Faraday Discuss.* **1997**, *106*, 41.

(23) Hill, J.-R.; Freeman, C.; Delley, B. *J. Phys. Chem. A* **1999**, *103*, 3772.

(24) Beck, K.; Pfeifer, H.; Staudte, B. *Microporous Mater.* **1993**, *2*, 1.

(25) Grünert, W.; Schlögl, R.; Karge, H. *J. Phys. Chem.* **1993**, *97*, 8638.

(26) Grünert, W.; Muhler, M.; Karge, H. *J. Chem. Soc., Faraday Trans.* **1996**, *92*, 701.

(27) Grünert, W.; Muhler, M.; Schröder, K.-P.; Sauer, J.; Schlögl, R. *J. Phys. Chem.* **1994**, *98*, 10920.

(28) Barr, T. L.; Lishka, M. *J. Am. Chem. Soc.* **1986**, *108*, 3178.